https://doi.org/10.5194/wes-2026-121
Preprint. Discussion started: 4 September 2026

eawe european academy of wind energy
Open Access WIND ENERGY SCIENCE DISCUSSIONS

Operational Weather Windows for Offshore Wind in the Taiwan Strait: Long-Term Variability, Regional Wind Modes, and Climate Linkages

Yi-Hui Wang[1], Yi-Chi Wang[2], Wan-Ling Tseng[3,*], Yueh-Shyuan Wu[4]

[1]Department of Statistics, California Polytechnic State University, San Luis Obispo, California, USA

[2]Swedish Meteorological and Hydrological Institute, Norrkoping, Sweden

[3]Institute of Sustainable Development and Climate Policy, National Tsing Hua University, Hsinchu, Taiwan

[4]Green Energy and Environment Research Laboratories, Industrial Technology Research Institute, Hsinchu, Taipei, Taiwan

*Corresponding Author: Wan-Ling Tseng, wltseng@mx.nthu.edu.tw

Abstract

Previous studies have either focused on shorter operational records or on ENSO-related variability over more limited periods, leaving the role of regional wind modes and longer-term climate context less explored. Here, we use more than 60 years of ERA5 reanalysis data to examine weather-window variability relevant to Taiwan's offshore wind development and to identify the proximal regional wind modes and large-scale climate linkages associated with this variability. Compared with winter, summer provides the greatest number of operational weather windows and exhibits relatively stable year-to-year variability, making it the primary season for offshore operational activities near Taiwan. Interannual variability in June-July-August mean weather-window counts is dominated by two regional wind modes across the Taiwan Strait, with secondary contributions from episodic tropical cyclone activity and broader climate linkages involving the Western North Pacific summer monsoon and ENSO-related sea surface temperature signal. Together, the regional wind modes, tropical cyclone activity, and climate-linkage indicators account for more than 60% of the variance in summer weather-window availability. Notably, during the period corresponding to the onset of Taiwan's offshore wind development (2018 - 2024), summers exhibited near-maximum accessibility relative to other 7-year windows in the 65-year record, indicating that such favorable conditions should not be assumed to persist. These results demonstrate the value of long-term weather-window analysis for addressing how offshore wind operating conditions are associated with broader climate variability and for supporting risk-informed construction and operations planning.

https://doi.org/10.5194/wes-2026-121
Preprint. Discussion started: 4 September 2026

1. **Introduction**

To mitigate greenhouse gas emissions, countries worldwide are accelerating the transition from fossil fuels to renewable energy. Among renewable sources, offshore wind (OSW) has emerged as a cornerstone of global decarbonization strategies. By the end of 2024, global OSW capacity reached approximately 83 GW (Global Wind Energy Council, 2025), with Taiwan among approximately twenty countries expanding this sector. In pursuit of a net-zero carbon future, the Taiwanese government has committed to installing 13.1 GW of OSW capacity by 2030 and between 40 and 55 GW by 2050 (National Development Council Taiwan, n.d.).

The eastern Taiwan Strait hosts most of the nation's existing and planned OSW projects (Fig. 1a & 1b), owing to its favorable wind resources, suitable seabed conditions, and proximity to population centers. However, this region also experiences substantial weather variability across multiple timescales. Adverse weather can delay offshore construction and operations & maintenance (O&M) activities leading to cost overruns and safety risks. Consequently, identifying and predicting "weather windows" - periods of sufficiently mild weather conditions - has become essential for efficient project planning, logistics, and risk management.

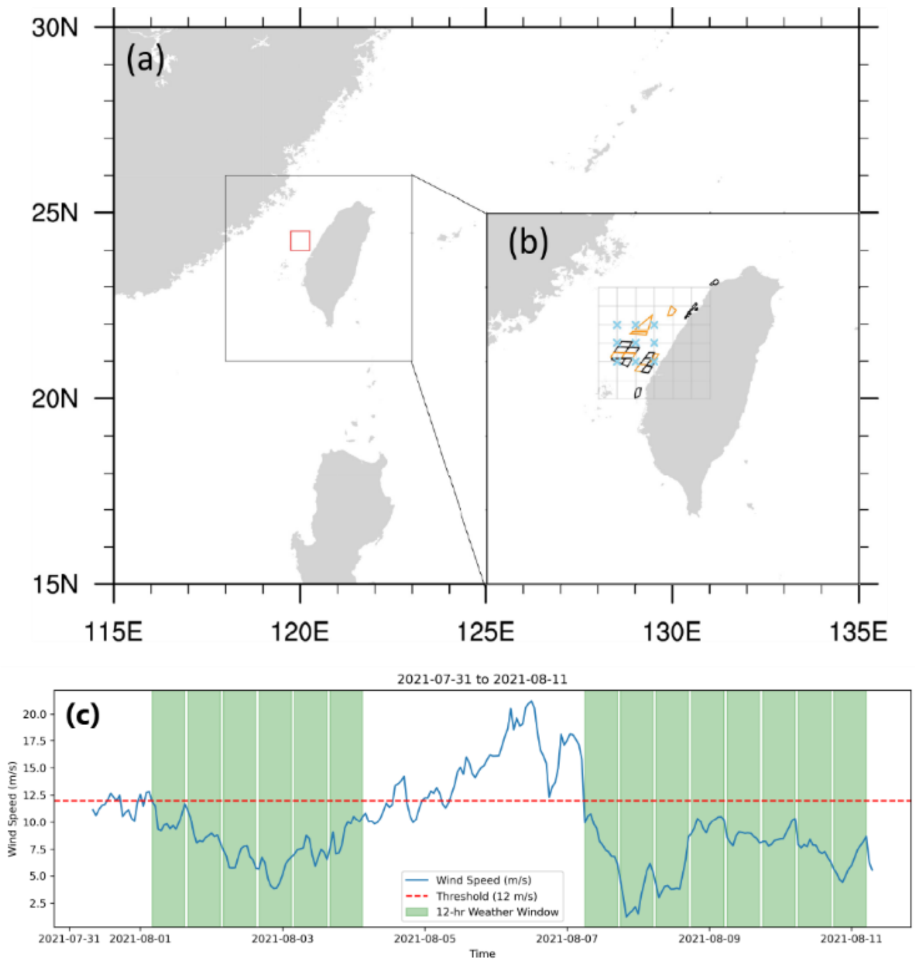

https://doi.org/10.5194/wes-2026-121
Preprint. Discussion started: 4 September 2026

Figure 1: (a, b) Locations of existing, under-construction, and potential future offshore wind (OSW) development areas in Taiwan. Black polygons denote operational OSW farms, and orange polygons indicate projects under construction at the time of publication in Tseng et al. (2024) (adapted from Tseng et al., 2024, licensed under CC BY-NC). (c) Example of 12-hour weather-window detections (green boxes) based on a 12 m s^{-1} threshold (red dashed line) applied to 100-m wind speed (blue curve) over a 10-day period.

Although numerous studies have characterized wind regimes in the Taiwan Strait for OSW development, most have emphasized the perspective of energy-production potential rather than operational accessibility (e.g., Hsu & Yeh, 2021). Far fewer have examined wind characteristics in the context of construction and O&M scheduling, especially at longer timescales beyond seasonality. If weather-window variability can be robustly characterized quantitatively, developers will be better positioned to allocate resources, schedule maintenance, and minimize downtime and costs ahead of time, thereby accelerating Taiwan's progress toward its energy targets.

Weather-window variability in the Taiwan Strait primarily reflects near-surface wind conditions shaped by interacting processes across timescales (Tseng et al., 2024). At diurnal and seasonal scales, winds are influenced by land-sea-breeze effects (Cheng et al., 2020) and monsoonal circulation, with stronger winds in winter than in summer (Shimada et al., 2016). Summer wind variability in the Taiwan Strait is linked to the large-scale Western North Pacific Summer Monsoon (WNPSM), which characterizes circulation anomalies across both tropical and subtropical regions of the western North Pacific. The WNPSM is closely linked to El Niño-Southern Oscillation (ENSO) variability, with warm-phase ENSO conditions in the preceding winter tending to weaken the WNPSM in the following summer (Wang et al., 2001).

During summer, tropical cyclones (TCs) can episodically influence environmental conditions and OSW operations in the Taiwan Strait. Typhoon-induced winds may temporarily increase power output to near turbine capacity (Ministry of Economic Affairs, R.O.C. (Taiwan), n.d.), but they also halt offshore activities during warning periods (W-L Tseng, personal communication, 2025).

Despite growing applications of weather-window analysis for offshore projects, the combined role of long-term variability, regional wind modes, and large-scale climate linkages remains insufficiently characterized for operational accessibility in the Taiwan Strait. This study addresses two main questions: (1) how do weather-window counts in Taiwan's OSW development areas vary across seasonal, interannual, and multi-decadal timescales, and (2) how are summer weather-window variations linked to regional wind modes, tropical cyclone activity, and large-scale climate indices? Quantifying these relationships provides an objective, climate-conditioned benchmark for evaluating offshore activity delays and planning deployment and maintenance timelines. Beyond the Taiwan Strait, this study demonstrates how long-term reanalysis data, regional wind-mode decomposition, and climate diagnostics can be combined to assess whether recent OSW operating conditions are representative of the broader climate distribution and to identify the regional and large-scale atmospheric patterns associated with operational accessibility.

https://doi.org/10.5194/wes-2026-121
Preprint. Discussion started: 4 September 2026

2. Data & Methods

2.1 Data

To capture lower-frequency variability, this study used data spanning 1960 - 2024. All wind data were obtained from the ERA5 reanalysis at a spatial resolution of 0.25° × 0.25° (Hersbach et al., 2020). Weather-window detection was based on hourly 100-m wind speed at 24° N, 120° E, representing the core area of Taiwan's OSW development in the Taiwan Strait. The 100-m level was selected following Tseng et al. (2024) to represent modern offshore hub heights and exhibits variability patterns consistent with 10-m winds. ERA5 100-m wind speeds at the study point were compared with 3-km wind fields produced by the Weather Research and Forecasting (WRF)-based data-assimilation system, developed by the Central Weather Administration of Taiwan, hereafter referred to as the CWA-WRF analyzed fields. Because these fields are constrained by local surface and radar observations through data assimilation (Chen et al., 2020), they provide higher-resolution regional wind information for Taiwan and serve as a useful regional benchmark for evaluating ERA5 rather than an independent observational dataset. We therefore use the comparison to assess ERA5's ability to capture regional and interannual variability, while observational support is provided by the wind-tower comparison reported in Tseng et al. (2024). Full comparison details, including bias quantification and weather-window count comparison, are provided in the Supplementary Material (Fig. S1).

Significant wave height data were also obtained from ERA5 at the same grid point to evaluate the sensitivity of weather-window definitions to combined wind–wave criteria; this analysis is presented in the supplementary material (Fig. S2). Tidal current and wave-period data were not considered because their influence on accessibility is secondary compared with wind speed and significant wave height (Moore et al., 2024).

Large-scale climate variability was represented using WNPSMI and the Oceanic Niño Index (ONI). WNPSMI was calculated from ERA5 monthly 850-hPa zonal winds as the difference between area-mean westerly winds in a southern box (5° - 15° N, 100° - 130° E) and a northern box (20° - 30° N, 110° - 140° E) following Wang et al. (2001). ENSO was quantified using the ONI, defined as the three-month running mean of sea surface temperature (SST) anomalies in the Niño 3.4 region (5° N - 5° S, 120° - 170° W), obtained from NOAA's Climate Prediction Center (n.d.). Monthly ERA5 850-hPa zonal and meridional winds and SST fields in JJA were also used for the spatial regression diagnostics linking PC2 to lower-tropospheric circulation and Pacific SST anomaly patterns.

To assess the influence of TCs, all unique TCs with centers recorded within a 4° × 4° domain centered at 24° N, 120° E (22° - 26° N, 118° - 122° E) were counted. Observations were obtained from the International Best Track Archive for Climate Stewardship (IBTrACS v4r01) maintained by NOAA's National Centers for Environmental Information (n.d.). Reliable TC records in the western North Pacific extend back to about 1945 (Knapp et al., 2010).

2.2 Weather Window Definitions

A weather window refers to a continuous period of sufficiently mild weather conditions allowing safe offshore operations. Key metrics shown in this study include:

https://doi.org/10.5194/wes-2026-121
Preprint. Discussion started: 4 September 2026

- Weather-window count: number of discrete periods meeting threshold criteria.
- Accessibility: fraction of total time when thresholds are met.

Because both metrics quantify the occurrence of continuous calm wind conditions, they are highly correlated.

Thresholds vary depending on activity type and vessel capability (Table S1). For example, crew transfer vessels typically have smaller wind limits than vessels for cable installations. Additionally, different levels of repairs require different weather window durations. As Rowell et al. (2022) addressed, a medium repair requires 7 - 24-hour weather window lengths, and a major repair needs at least 24 hours. This study followed Tseng et al. (2024), which defined a weather window as 100-m wind speed < 12 m s^{-1} for 12 consecutive hours. If the condition persisted for an additional 12 hours, a second weather window was counted; if winds exceeded the threshold between 13 - 24 hours, the count reset (Fig. 1c). When a window spanned two months, its duration was apportioned proportionally to each month.

Because monthly weather-window counts based on wind speed alone are highly correlated with those derived from combined wind-wave criteria ($r > 0.98$; Fig. S2), subsequent analyses adopt the 12 m s^{-1} 100-m wind-speed threshold sustained for 12 consecutive hours as a representative measure of weather-window variability.

To assess whether the study point is spatially representative of the broader OSW development zone, monthly weather-window counts were computed at the eight surrounding ERA5 grid points (0.25° spacing) and compared against the study point series for 1960 - 2024. Except for the southeastern neighbor, which sits primarily over the western plains of Taiwan and falls outside the primary OSW development zone, all the remaining seven neighbors have annual R^2 values exceeding 0.96, confirming that the climate-driven variability examined in this study is spatially coherent across the OSW development region (not shown).

2.3 EOF analysis

Empirical Orthogonal Function (EOF) analysis (Wilks, 2011) was applied to summer-mean (June-July-August, JJA) 100-m wind-speed hourly anomalies, which are defined as hourly departures from each month's climatological mean, averaged across all hours of JJA, within the 4° × 4° domain centered at 24° N, 120° E to identify dominant spatial and temporal modes of regional wind variability. This approach allows persistent seasonal departures associated with recurrent synoptic variability to contribute to the annual JJA anomaly field.

2.4 Cross-Validation and Multicollinearity

To evaluate whether model skill generalizes beyond the training period, the leave-one-out cross-validation (LOOCV) method was applied. The exchangeability assumption underlying the LOOCV was assessed by applying the Ljung-Box test (Ljung and Box, 1978) at lags 1–5 to the residuals of the regression model containing all predictors (the full model in Fig. 6). No significant autocorrelation was detected at lags 1-5 for any series ($p > 0.05$), confirming that annual JJA means are approximately independent year to year and that standard LOOCV withholding one year at a time constitutes a valid independent test. The LOOCV method iteratively withheld one year at a time, trained the model on the remaining 64 years,

https://doi.org/10.5194/wes-2026-121
Preprint. Discussion started: 4 September 2026

and predicted the withheld year; R^2 was computed globally across all predictions. Together these approaches assess both the temporal stability and the year-to-year generalizability of the regression models.

Correlated predictors in a multiple linear regression model can produce multicollinearity, which destabilizes regression coefficients and inflates standard errors, reducing the precision of estimates. The severity of multicollinearity was assessed using the variance inflation factor (VIF) for each predictor. A VIF exceeding 4 was used as the threshold for flagging potential instability, following standard practice (O'Brien, 2007).

2.5 Statistical Pathway Decomposition

Predictors were entered hierarchically in order of their bivariate correlation magnitude with JJA weather-window counts, reflecting their direct statistical association prior to controlling for other variables. Given the correlation of PC2 with WNPSMI and ONI, we conducted mediation analysis following Baron and Kenny (1986) to examine whether PC2 provides a statistical indirect pathway linking WNPSMI and ONI to weather-window variability. The mediation pathway was decomposed into a total effect (c), an indirect effect via PC2 ($a \times b$), and a direct effect (c'). The significance of the indirect effect ($a \times b$) was assessed using a bootstrap procedure (Efron & Tibshirani, 1993) with 10,000 resamples. A 95% bootstrap confidence interval for the indirect effect that excludes zero is taken as evidence of a bootstrap-supported indirect pathway.

2.6 Physical Regression Diagnostics

To interpret the regional wind modes physically, we regressed seasonal anomaly fields onto the corresponding PC time series. Data were first averaged to obtain annual JJA means, and the 1960-2024 JJA climatology was removed at each grid cell to obtain seasonal anomalies. The anomalies were then separately regressed onto the relevant PC time series using the least squares approach. PC amplitudes were used in their native EOF scaling, so regression coefficients are reported per unit PC amplitude. Pointwise p-values were calculated from the regression t-test and are shown only as local significance indicators. The 850-hPa wind and SST regressions were used to diagnose the WNPSM-related circulation and ENSO-related SST context of PC2. Additional 100-m vector-wind regressions onto PC1 were conducted as a supporting diagnostic of near-surface flow geometry and are presented in the supplemental material (Fig. S3).

3. Results

3.1 Temporal Variability Weather Windows

We first examine the seasonal cycle of weather-window availability. Weather-window counts vary substantially by month, with the greatest availability occurring in summer when 100-m wind speeds are weakest (Fig. 2). From April to September, the mean number of 12-hour weather windows typically exceeds 40 per month, more than twice the winter values. Warm-season months also exhibit smaller interannual variability, as indicated by the narrower standard-deviation ranges compared with cold-season months. Because JJA provides the highest operational accessibility while still retaining meaningful year-to-year variability, the subsequent analysis focuses on summer weather-window variability.

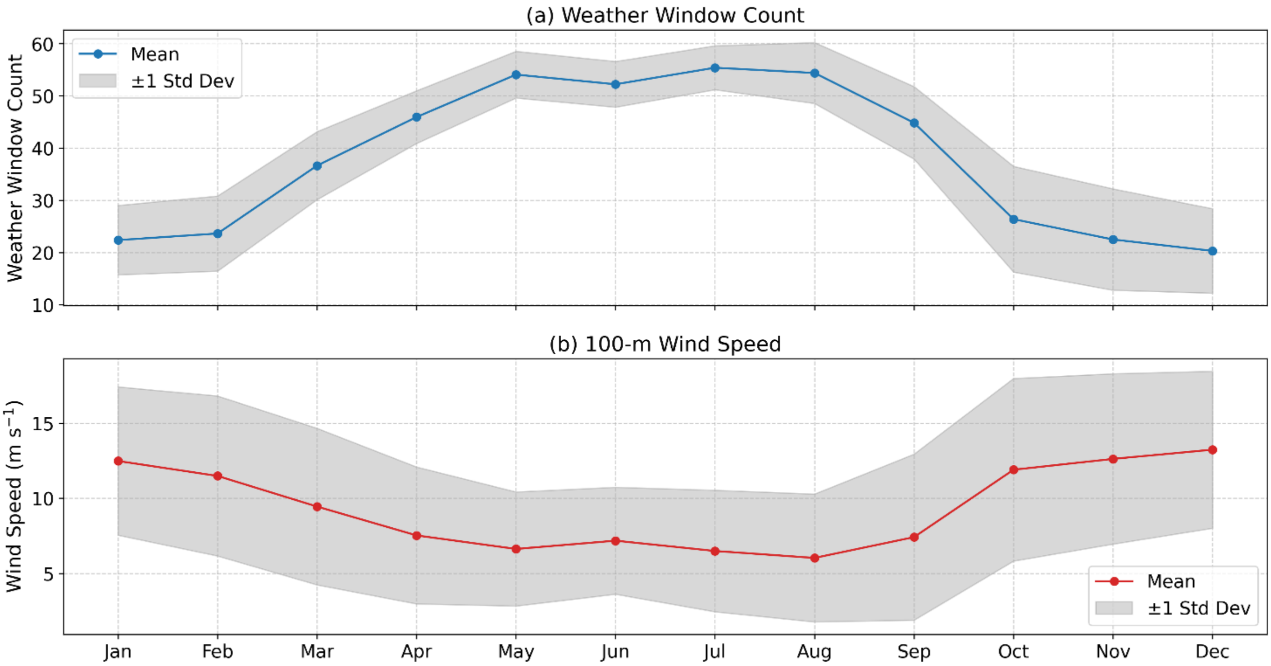

Figure 2: Monthly means (solid lines) and ±1 standard deviation (shaded areas) of (a) 12-hour weather-window counts and (b) 100-m wind speed at 24° N, 120° E over 1960-2024.

185

Given that Taiwan's large-scale OSW construction began around 2018, it is essential to evaluate whether recent calm conditions are typical of historical variability. Figure 3 compares mean accessibility during 2018 - 2024 against all 59 overlapping 7-year windows in the 1960 - 2024 record, with blue bars showing the percentile of the 2018 - 2024 mean among these historical 7-year windows. It shows that recent summers (June - August) exceeded the long-term median, while

190 December ranked among the lowest historical percentiles. These results suggest that recent operational conditions have been more favorable than climatological norms in summer but less favorable in winter.

https://doi.org/10.5194/wes-2026-121
Preprint. Discussion started: 4 September 2026

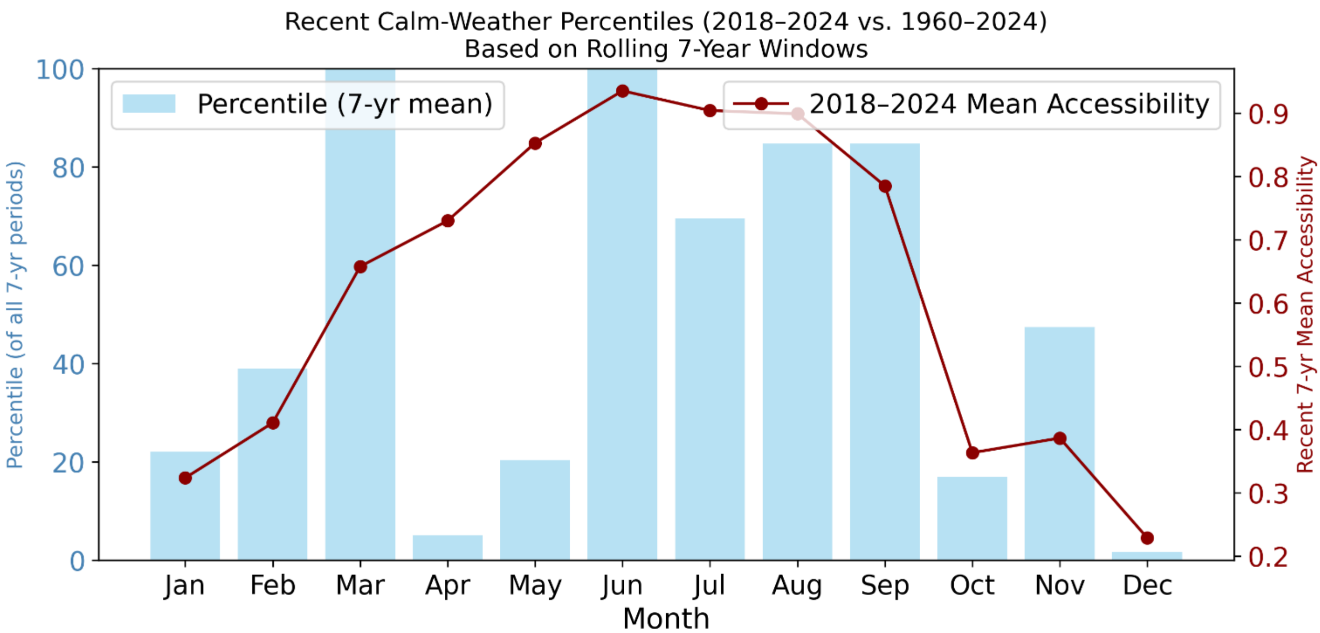

Figure 3: Monthly mean accessibility during 2018-2024 (red curve) and its percentiles (blue bars) from all 7-year running periods between 1960 and 2024.

3.2 Summer Climate Linkages and Regional Wind Modes

Given that summer offers more operational weather windows and exhibits relatively stable interannual variability compared with winter, we focus on the interannual variability of mean JJA weather-window counts and examine their relationships with WNPSMI, ONI, and TC frequency for 1960–2024 (Table 1). All three indices show moderate but statistically significant negative correlations with weather-window counts, consistent with the physical expectation that intensified monsoon circulation, El Niño conditions, and higher TC activity all strengthen winds and reduce calm-condition frequency.

Table 1: Correlation matrix among key variables: JJA-mean weather-window counts (WW), leading and secondary principal components of the first two EOF wind modes (PC1 and PC2), Western North Pacific Summer Monsoon Index (WNPSMI), Oceanic Niño Index (ONI), and tropical-cyclone frequency (TC Freq). *** indicates statistical significance with p-value < 0.001, ** p < 0.01, * p-value < 0.05.

	WW	PC1	PC2	WNPSMI	ONI	TC Freq
WW	1	-0.58***	0.49***	-0.35**	-0.29*	-0.36**
PC1		1	~0	0.09	0.11	0.15
PC2			1	-0.4**	-0.33**	-0.12

https://doi.org/10.5194/wes-2026-121
Preprint. Discussion started: 4 September 2026

WNPSMI				1	0.34**	0.23
ONI					1	-0.07
TC Freq						1

While previously considered indices show moderate associations with the summer weather window interannual variability, additional patterns may arise from regional or local wind dynamics. As Fig. 4 shows, the correlation between the JJA-mean hourly 100-m wind speed anomalies and weather-window counts reaches as low as -0.74 across much of the Taiwan Strait with statistical significance ($p < 0.01$), consistent with the physical expectation that stronger wind events reduce operational weather windows. To identify the dominant spatial and temporal modes characterizing weather window variability, EOF analysis was applied to JJA-mean hourly 100-m wind-speed anomalies within the 4° × 4° domain.

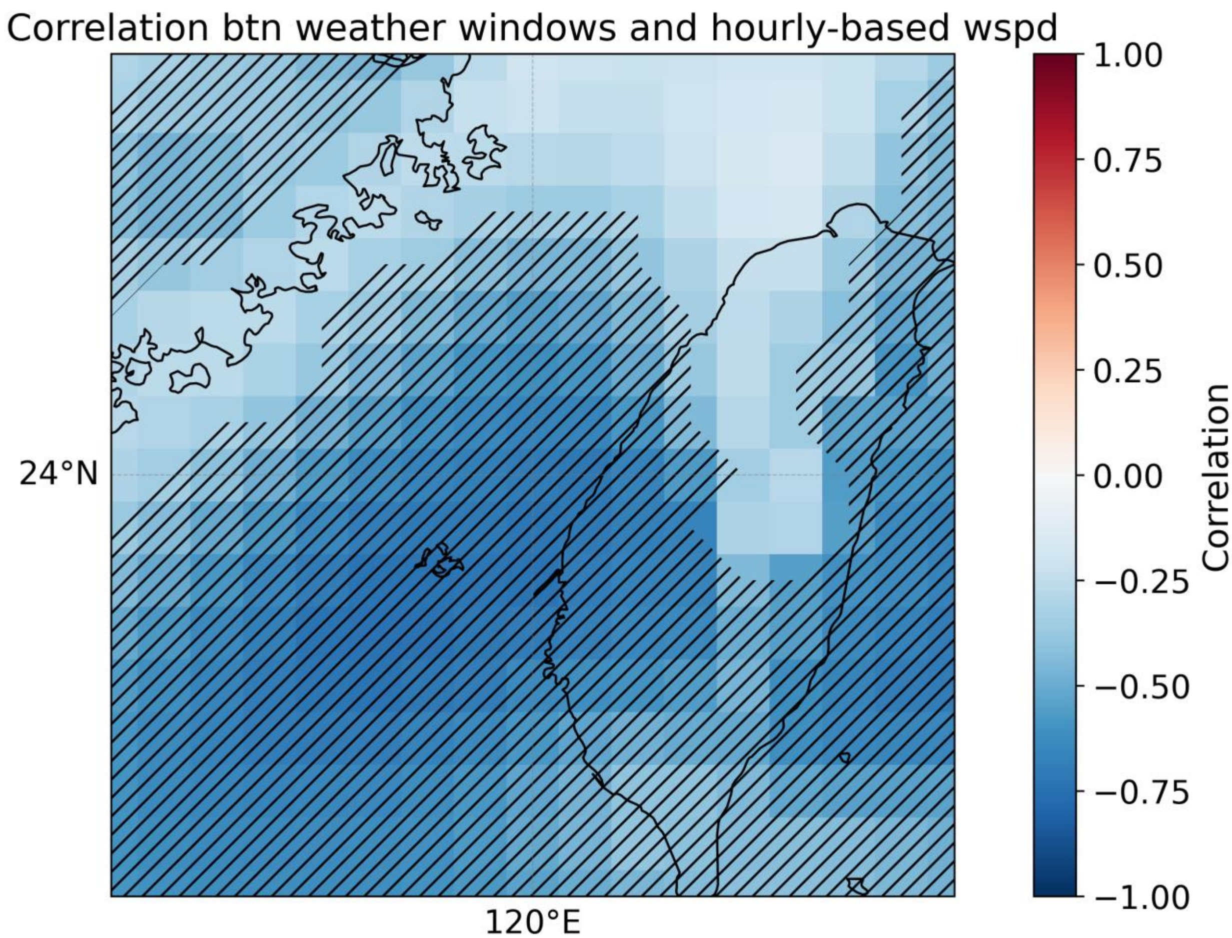

https://doi.org/10.5194/wes-2026-121
Preprint. Discussion started: 4 September 2026

Figure 4: Correlation between JJA-mean weather window counts and JJA-mean hourly 100-m wind speed anomalies for 1960-2024. Hatched areas show statistical significance at p-value < 0.01.

Figure 5 shows that the leading two modes explain approximately 77.5 % of total variance. EOF1, accounting for > 60 % of variance, represents a coherent strengthening of winds across the central Taiwan Strait; its corresponding time coefficient (PC1) correlates strongly and negatively with weather-window counts (r = -0.58) (Table 1). EOF2 exhibits a north-south dipole structure, associated with meridional shifts in wind intensity, and correlates positively with weather-window counts (r = 0.49) (Table 1). Together, these modes highlight that local and regional wind variability - especially the first mode - plays a more direct role in controlling operational accessibility than large-scale indices alone.

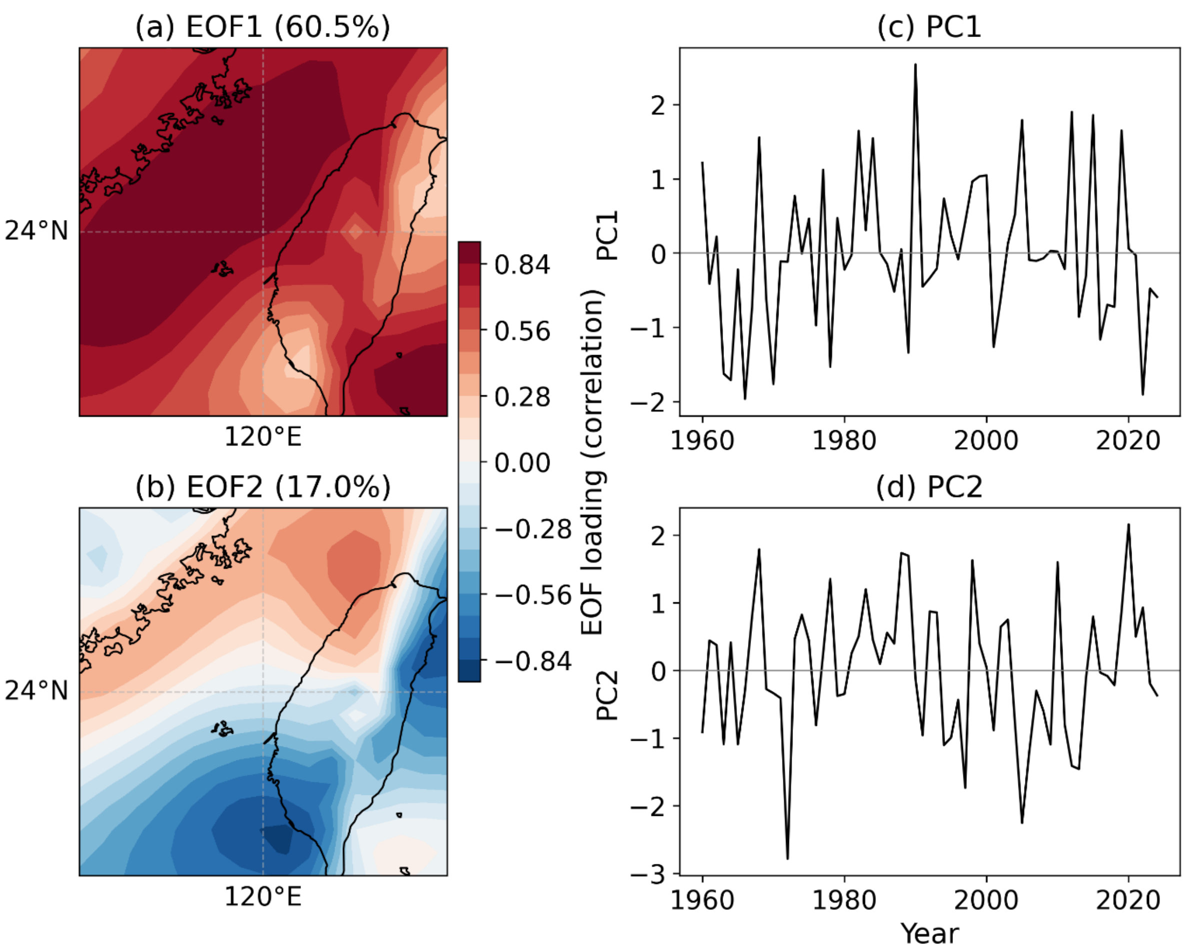

Figure 5: Spatial patterns of EOF1 (a) and EOF2 (b) and their corresponding principal component time series, PC1 (c) and PC2 (d), derived from JJA-mean hourly wind-speed anomalies over 1960 - 2024.

https://doi.org/10.5194/wes-2026-121
Preprint. Discussion started: 4 September 2026

Among the variables considered, PC1 and PC2 show the strongest associations with JJA weather-window counts, but they represent a different type of predictor than the large-scale climate indices. Because PC1 and PC2 are regional wind modes derived from the Taiwan Strait wind field, they describe the proximal wind structures most directly linked to operational accessibility. In contrast, WNPSMI, ONI, and TC frequency represent large-scale climate variability or episodic storm activity that may influence weather windows through their effects on the regional wind field. We therefore used hierarchical modeling to evaluate the relative explanatory contributions of the regional wind modes, TC activity, and large-scale climate indices to summer weather-window variability.

3.3 Model Hierarchy and Contributions to Summer Weather Window Variability

Five hierarchical models were developed to quantify the incremental explanatory power of the regional wind modes, TC frequency, and large-scale climate indices. Predictors were entered in order of their correlations with weather-window counts; this ordering is intended to evaluate added explanatory power rather than imply causal priority. As summarized in Fig. 6, Model 1, which includes PC1 only, explains 34% of the variance in JJA weather-window counts. Adding PC2 in Model 2 increases the explained variance to 58%, a gain of 24 percentage points, indicating the substantial additional contribution of the north–south dipole wind structure beyond the coherent wind-speed mode captured by PC1. Model 3 adds TC frequency and increases R^2 to 63%, although its incremental contribution is much smaller than that of PC2. Models 4 and 5 add WNPSMI and ONI, respectively, and provide only marginal additional gains in explanatory power ($\Delta R^2 = 0$ and 0.01, respectively).

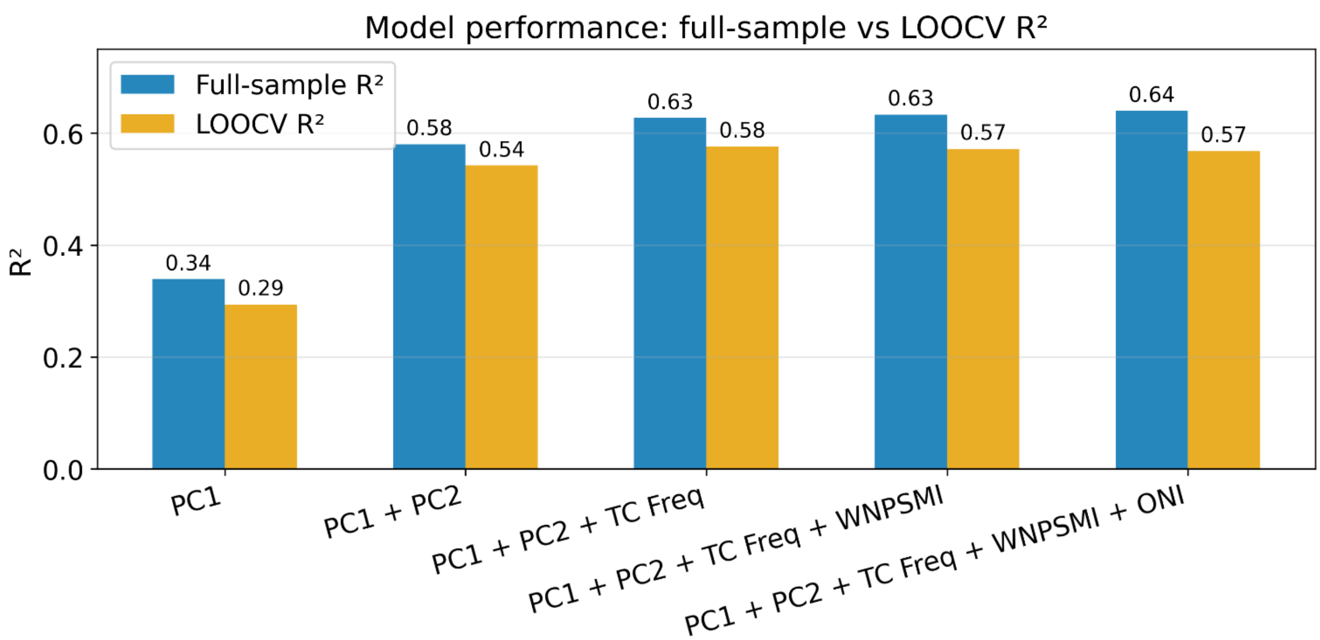

Figure 6: Hierarchical regression model performance for JJA mean weather-window counts at 24° N, 120° E. Blue bars show full-sample R^2 for models trained on the complete 1960-2024 record. Orange bars show leave-one-out cross-validation (LOOCV) R^2 computed across all 65 years. The five models add predictors sequentially: regional wind modes (PC1, PC2), tropical cyclone frequency (TC Freq), Western North Pacific Summer Monsoon Index (WNPSMI), and Oceanic Niño Index (ONI).

Although these hierarchical models are intended to characterize historical variance rather than provide an operational forecast, LOOCV was used to assess whether the identified relationships generalize beyond the training sample. The cross-validated R^2 values are slightly lower than the in-sample R^2 values, but they preserve the same model hierarchy: PC1 and PC2 provide the dominant explanatory power, TC frequency adds a smaller contribution, and WNPSMI and ONI provide little additional skill once the regional wind modes and TC activity are included. In the full model, WNPSMI and ONI have non-significant regression coefficients, indicating that their bivariate associations with weather-window counts do not translate into strong independent explanatory power in the multivariable model. This result is not attributable to severe multicollinearity, as all VIF values are below 4 and low (PC1 = 1.04, PC2 = 1.27, TC Freq = 1.12, WNPSMI = 1.34, ONI = 1.25). The next section therefore examines whether these large-scale climate-index associations are instead expressed through the PC2 regional wind-dipole mode.

3.4 PC2-Associated Climate-Index Pathways

Because WNPSMI and ONI are both correlated with PC2 but add little independent explanatory power in the hierarchical models, we further decomposed their associations with weather-window counts into direct components and PC2-associated indirect pathways (Fig. 7). This analysis is interpreted as a statistical pathway decomposition rather than as evidence of causal mediation, because all variables are derived from observational climate variability.

After adjusting for PC1 and separating the WNPSMI and ONI pathways from their shared variability after controlling for the other index, the WNPSMI pathway is robust: WNPSMI was significantly associated with PC2, PC2 was strongly associated with weather-window counts, and the PC2-associated indirect pathway was negative and bootstrap-supported (indirect effect = -0.37; 95% bootstrap CI = -0.68 to -0.09). The remaining direct WNPSMI-weather-window association was not significant, indicating that much of the WNPSMI relationship with operational accessibility is expressed through the PC2 dipole mode.

ONI showed a similar sign structure but weaker independent evidence. The ONI-associated indirect pathway through PC2 was negative and its bootstrap confidence interval narrowly excluded zero (indirect effect = -0.38; 95% bootstrap CI = -0.88 to -0.003), but the total ONI-weather-window association, adjusted for PC1 and WNPSMI, was not significant and the ONI-PC2 path was only marginal. We therefore interpret the ONI pathway as suggestive rather than definitive. Together, these results indicate that the climate-index relationships with summer weather-window variability are better understood as climate linkages expressed through a regional wind-dipole mode, with stronger support for WNPSMI than for ONI. Additional

https://doi.org/10.5194/wes-2026-121
Preprint. Discussion started: 4 September 2026

WIND ENERGY SCIENCE DISCUSSIONS
Open Access

adjustment for TC frequency produced the same overall sign structure (not shown), supporting the robustness of the PC2-associated pathway.

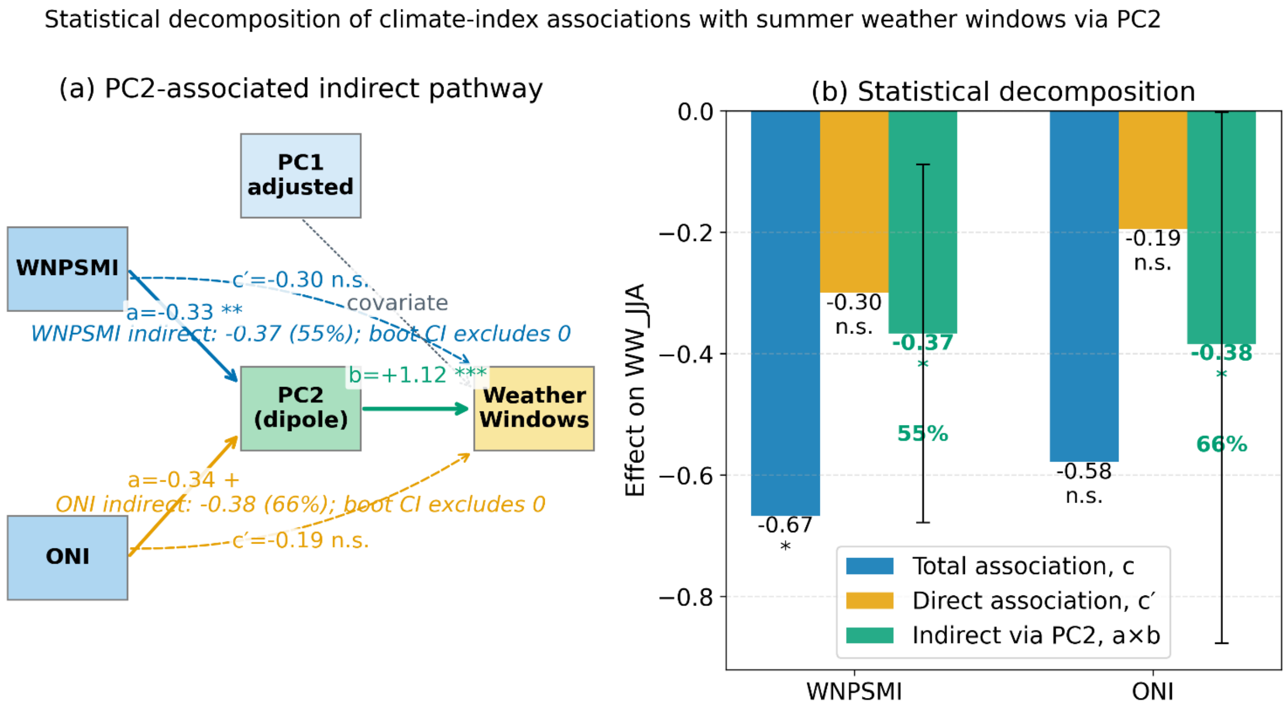

Figure 7: PC2-associated statistical pathway linking large-scale climate indices to summer weather-window counts. (a) Path diagram showing the pathway model, in which PC1 is included as a covariate and WNPSMI and ONI are mutually controlled for one another. (b) Total (blue), direct (orange), and indirect (green) effects of WNPSMI and ONI on weather-window counts, estimated from the model shown in (a); error bars on the indirect effect denote the bootstrap 95% confidence interval. Significance levels: *** $p < 0.001$, ** $p < 0.01$, * $p < 0.05$, + $p < 0.10$, n.s. $p \geq 0.10$.

3.5 Physical Context for PC2-Associated Climate Linkages

Given the statistical pathways associated with PC2 and climate indices identified earlier, the following regressions are used as physical diagnostics to test whether the regional wind modes are embedded within physically interpretable large-scale patterns.

According to Fig. 8, which shows the regression of JJA 850-hPa wind anomalies onto the PC2 time series, there is a clear contrast between the two WNPSMI definition regions with negative u850 anomalies in the southern box and positive u850 anomalies in the northern box when PC2 is positive. Box-averaged u850 regression coefficients are -0.57 m s^{-1} per unit PC2 in the southern box and +0.31 m s^{-1} per unit PC2 in the northern box, corresponding to an implied WNPSMI contrast of -0.88 m s^{-1} per unit PC2. The u850 regression is significant over 91% of grid cells in the southern box and 60% in the northern box at the pointwise $p < 0.05$. This pattern is consistent with the negative PC2 - WNPSMI correlation and indicates

https://doi.org/10.5194/wes-2026-121
Preprint. Discussion started: 4 September 2026

that positive PC2 years tend to coincide with a weaker WNPSMI-like lower-tropospheric zonal-wind contrast, while negative PC2 years tend to coincide with a stronger WNPSMI-like contrast. The 850-hPa wind regression therefore provides physical context for the robust PC2-associated WNPSMI pathway identified in the statistical decomposition.

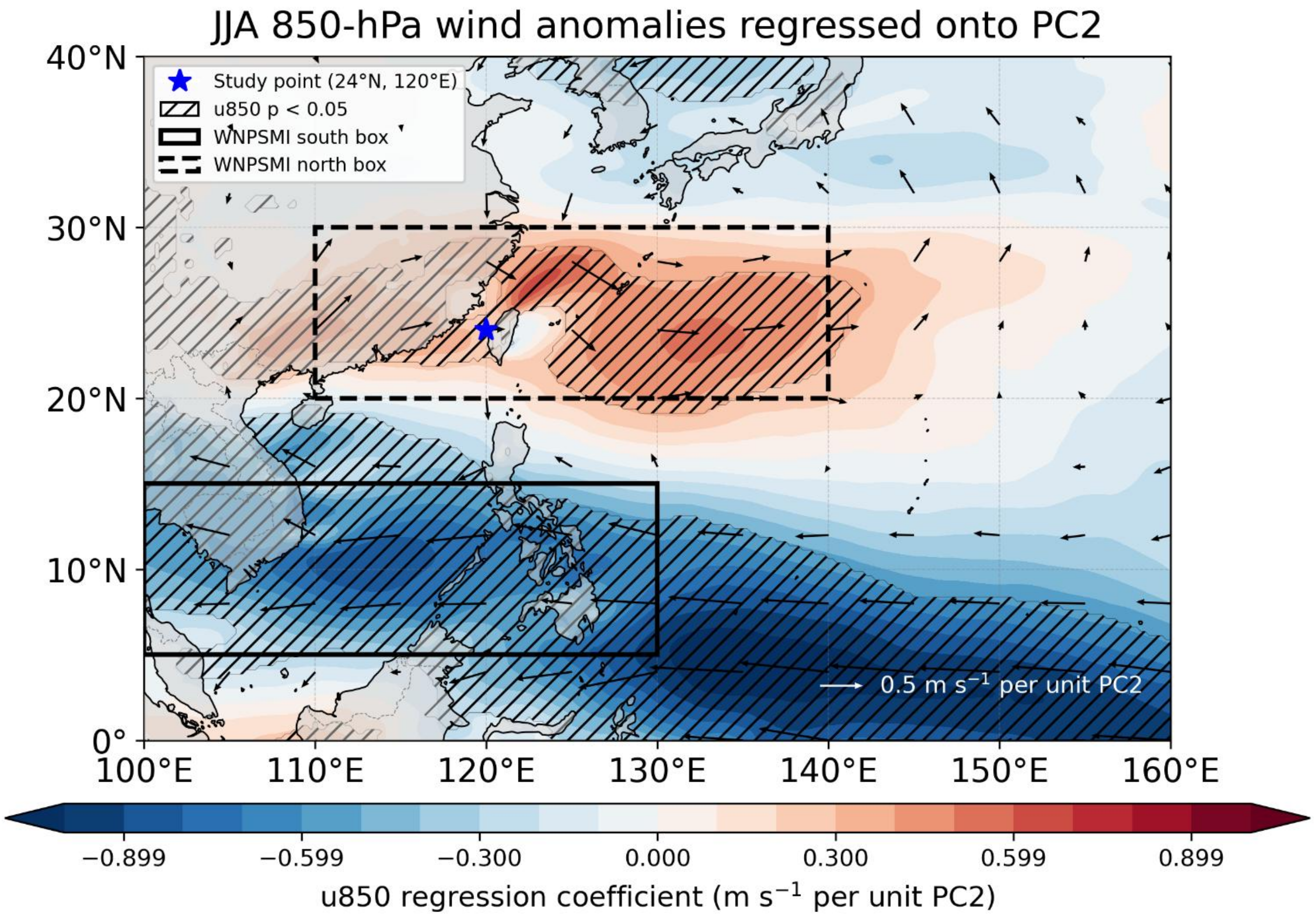

Figure 8. JJA 850-hPa wind anomalies regressed onto PC2 for 1960 - 2024. Shading shows the u850 regression coefficient in m s^{-1} per unit PC2, vectors show the combined u850 and v850 regression coefficients, and hatching denotes grid cells where the u850 regression is significant at the pointwise $p < 0.05$. The solid and dashed black boxes mark the southern and northern regions used to define WNPSMI, respectively, and the blue star marks the Taiwan Strait study point.

Although the PC2-ONI relationship is weaker than the PC2-WNPSMI relationship, we also examined whether PC2 is associated with an ENSO-like SST anomaly pattern through regression analysis (Fig. 9). While Wang et al. (2001) addressed preceding-winter ENSO effects on WNPSM, lagged ENSO influences on the following summer WNPSM are not separately attributed here. The resulting pattern shows negative regression coefficients across the Niño 3.4 region, indicating that

https://doi.org/10.5194/wes-2026-121
Preprint. Discussion started: 4 September 2026

positive PC2 years are associated with cooler central-eastern equatorial Pacific SST anomalies. Averaged over the Niño 3.4 box, the regression coefficient is -0.29 K per unit PC2, and 96% of grid cells within the box are significant at the pointwise $p < 0.05$. This pattern is consistent with the negative PC2-ONI correlation identified in the correlation analysis and suggests that El Niño-like conditions tend to coincide with the negative phase of PC2. Because negative PC2 is associated with reduced summer weather-window availability, the SST regression provides physical context for the weaker but suggestive ONI-associated pathway identified in the statistical decomposition. Outside the tropical Pacific, positive SST regression coefficients appear in parts of the western Pacific, but the Taiwan Strait region itself does not show a statistically significant SST relationship. Therefore, the SST evidence is best interpreted as support for a broad ENSO-related linkage to PC2 rather than as evidence of a local SST control on Taiwan Strait weather-window variability.

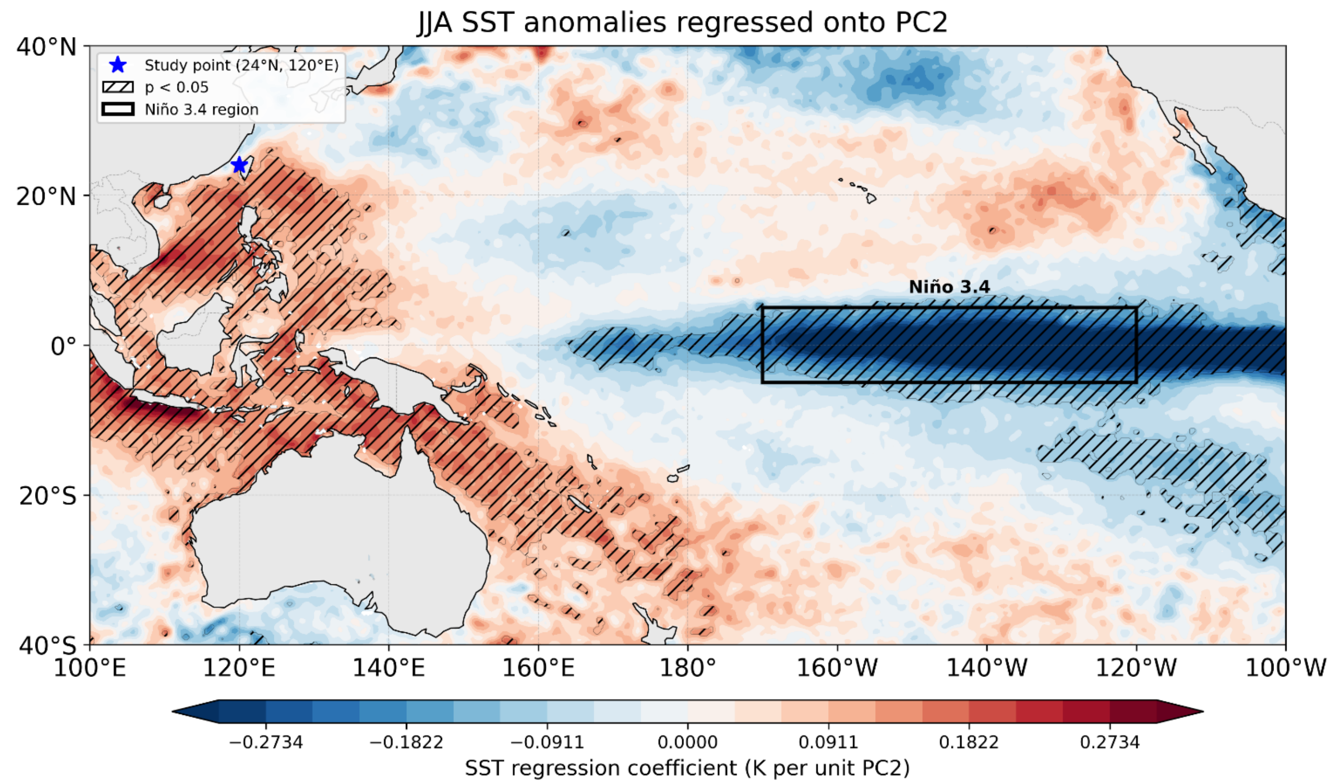

Figure 9. JJA SST anomalies regressed onto PC2 for 1960 - 2024. Shading indicates the SST regression coefficient in K per unit PC2, and hatching denotes grid cells significant at the pointwise $p < 0.05$. The black box marks the Niño 3.4 region used to define the Oceanic Niño Index, and the blue star marks the Taiwan Strait study point. Negative regression coefficients within the Niño 3.4 region indicate that positive PC2 years are associated with cooler central-eastern equatorial Pacific SST anomalies, while negative PC2 years are associated with warmer Niño 3.4 SST anomalies.

https://doi.org/10.5194/wes-2026-121
Preprint. Discussion started: 4 September 2026

While PC1 does not show significant correlation with climate indices, we regressed 100-m vector-wind field onto PC1 and found that PC1 is accompanied by near-surface flow anomalies spatially consistent with terrain-modified flow around Taiwan's Central Mountain Range, although this diagnostic should not be interpreted as an independent attribution of PC1 to topographic forcing (Fig. S3).

4. Conclusions and Discussions

This study provides a 65-year assessment of offshore operational weather windows in the Taiwan Strait. Weather-window availability is strongly seasonal, with summer providing substantially more 12-hour windows than winter. The seasonal cycle shows that summer provides the most favorable operational conditions, motivating a focused analysis of JJA interannual variability and its regional wind-mode and climate linkages. We found that summer weather-window variability is controlled primarily by two regional wind modes. PC1 represents coherent wind-speed variability across the Taiwan Strait and alone explains 34% of JJA weather-window variance. PC2 represents a north-south dipole mode and increases the explained variance to 58% when added to PC1. TC frequency provides a smaller but unignorable contribution, increasing explained variance to approximately 63% and indicating that episodic storm activity remains an important constraint on summer accessibility.

Large-scale climate indices provide important context but limited independent explanatory power once the regional wind modes are included. WNPSMI and ONI are both associated with PC2, and statistical pathway decomposition indicates that their relationships with summer weather-window counts are expressed primarily through the PC2 dipole mode rather than through independent direct associations. This PC2-associated pathway is robust for WNPSMI and weaker, but suggestive, for ONI after mutual adjustment. The regressions show that PC2 is associated with a WNPSMI-like 850-hPa zonal-wind contrast and, more weakly, with an ENSO-like tropical Pacific SST anomaly pattern. These diagnostics support the physical interpretation that large-scale climate variability is associated with Taiwan Strait weather-window variability primarily through regional wind-field expression rather than through direct independent effects. These results highlight the importance of distinguishing proximal regional wind modes, which directly structure operational accessibility, from broader climate indices, which provide large-scale context for those regional patterns.

Recent summers during 2018-2024 were more favorable than much of the historical record, indicating that early OSW development in the Taiwan Strait occurred during relatively accessible summer conditions that should not be assumed to persist. Together, these findings demonstrate the value of using long-term climate records to benchmark OSW accessibility, distinguish regional wind controls from broader climate linkages, and support risk-informed planning for construction and O&M activities.

Several limitations should be considered when interpreting these results. First, the primary analysis of this study uses weather windows defined by a representative 100-m wind-speed threshold and does not capture all vessel-, task-, or contractor-specific operating constraints. Second, the EOF modes are derived from the same regional wind field used to calculate weather-window counts, so they should be interpreted as proximal wind-field descriptors rather than independent

https://doi.org/10.5194/wes-2026-121
Preprint. Discussion started: 4 September 2026

external drivers. Finally, the physical regressions provide diagnostic consistency with monsoon and ENSO patterns but do not constitute formal attribution experiments.

This study relies primarily on ERA5 because it provides the long, hourly, spatially complete 100-m wind record needed to evaluate multi-decadal weather-window variability. Prior comparison with wind-tower observations and the CWA-WRF analyzed fields by Tseng et al. (2024) supports ERA5's ability to capture regional wind variability, and our Supplementary Material shows high interannual agreement in weather-window counts. However, ERA5 underestimates wind speed relative to the higher-resolution CWA-WRF analyzed fields and overestimates absolute weather-window counts; therefore, absolute accessibility values should be interpreted with caution. We did not repeat the full analysis using alternative global reanalyses, so the sensitivity of the detailed EOF patterns and quantitative coefficients to reanalysis choice remains a topic for future work.

This analysis is not intended to provide an operational forecast model. Instead, it provides a climate-conditioned baseline against short-term observations, which is important for OSW planning. While short records may capture recent favorable or unfavorable periods, they cannot determine whether those conditions are representative of the broader climate distribution. By combining a 65-year weather-window record with regional wind-mode analysis and climate-index linkages, this study provides a framework for identifying how weather-window variability emerges from both regional wind-field controls and broader climate context. While the Taiwan Strait results are site-specific, the framework is transferable: long-term weather-window characterization, regional wind-mode decomposition, hierarchical contribution analysis, and climate-linkage diagnostics can be applied to other offshore wind regions where long wind records are available. Future work could extend this framework by incorporating vessel-specific thresholds, additional wave and current constraints, workability requirements for different offshore activities, and probabilistic seasonal prediction tools.

Data availability

The data that supports the findings of this study are openly available. ERA5 reanalysis data can be accessed via the Copernicus Climate Data Store (https://cds.climate.copernicus.eu/). CWA-WRF analyzed fields used for comparison with ERA5 are not publicly available; access is restricted under the agency's data sharing policy. Information on other indices used in this study is provided in the Data and References. Derived data generated during this study are available from the corresponding author upon reasonable request.

Code availability

The Python scripts used for statistical analysis and figure generation are available upon reasonable request. Scripts that use the CWA-WRF analyzed fields (Sect. 2.1, Fig. S1) additionally require separate access to that restricted dataset before they can be run; see the Data availability statement for details.

Author contributions

YHW, YCW, and WLT contributed equally to conceptualization. YHW performed the formal analysis, created the visualizations, and wrote the original draft. YHW, YCW and WLT reviewed and edited the manuscript. WLT supervised the project and acquired funding. WLT and YSW administered the project. YSW also provided funding agency's feedback and industry insight.

Acknowledgments

Generative AI tools (Claude, Anthropic) were used to assist in writing portions of the Python code used for data analysis and figure generation, and to assist with manuscript language polishing. All code was reviewed, tested, and verified by YHW. We also thank the National Center for High-Performance Computing, National Institutes of Applied Research (NIAR), Taiwan, for providing academic computing resources and infrastructure.

Financial support

This study was supported by the Industrial Technology Research Institute in Taiwan for the project "Assessment of the Influence of Decadal Oscillations on Wind Speeds and Weather Windows for Offshore Wind Power System Installation in the Taiwan Strait". Additional funding was provided by the National Science and Technology Council under grant numbers NSTC 113-2111-M-002-016, 114-2628-M-002-015-MY4, 112-2923-M-001-003-MY4.

References

Baron, R. M. and Kenny, D. A.: The moderator–mediator variable distinction in social psychological research: conceptual, strategic, and statistical considerations, J. Pers. Soc. Psychol., 51, 1173–1182, https://doi.org/10.1037/0022-3514.51.6.1173, 1986.

Chen, I.H., Hong, J.-S., Tsai, Y.-T., and Fong, C.-T.: Improving Afternoon Thunderstorm Prediction over Taiwan through 3DVar-Based Radar and Surface Data Assimilation, Weather and Forecasting 35, 2603-2620, https://doi.org/10.1175/WAF-D-20-0037.1, 2020.

Cheng, K.-S., Ho, C.-Y., and Teng, J.-H.: Wind characteristics in the Taiwan Strait: a case study of the first offshore wind farm in Taiwan, Energies, 13, 6492, https://doi.org/10.3390/en13246492, 2020.

Efron, B. and Tibshirani, R.: An Introduction to the Bootstrap, Chapman and Hall, New York, 1993.

Global Wind Energy Council: Global Offshore Wind Report 2025, Global Wind Energy Council, available at: https://www.gwec.net/reports/globaloffshorewindreport/2025 (last access: 26 January 2026), 2025.

Hersbach, H., Bell, B., Berrisford, P., Hirahara, S., Horányi, A., Muñoz-Sabater, J., Nicolas, J., Peubey, C., Radu, R., Schepers, D., Simmons, A., Soci, C., Abdalla, S., Abellan, X., Balsamo, G., Bechtold, P., Biavati, G., Bidlot, J., Bonavita,

https://doi.org/10.5194/wes-2026-121
Preprint. Discussion started: 4 September 2026

M., ... Thépaut, J.-N.: The ERA5 global reanalysis, Q. J. Roy. Meteor. Soc., 146, 1999–2049, https://doi.org/10.1002/qj.3803, 2020.

Hsu, W.-K. and Yeh, C.-K.: Offshore wind potential of west central Taiwan: a case study, Energies, 14, 3702, https://doi.org/10.3390/en14123702, 2021.

Knapp, K. R., Kruk, M. C., Levinson, D. H., Diamond, H. J., and Neumann, C. J.: The International Best Track Archive for Climate Stewardship (IBTrACS): unifying tropical cyclone data, B. Am. Meteorol. Soc., 91, 363–376, https://doi.org/10.1175/2009BAMS2755.1, 2010.

Ljung, G. M. and Box, G. E. P.: On a measure of lack of fit in time series models, Biometrika, 65, 297–303, https://doi.org/10.1093/biomet/65.2.297, 1978.

Ministry of Economic Affairs, R.O.C. (Taiwan): Taiwan's offshore wind turbines stand strong against Typhoon Danas, available at: https://www.moea.gov.tw/MNS/english/news/News.aspx?kind=6&menu_id=176&news_id=120300 (last access: 26 January 2026), n.d.

Moore, D., Eftekhari, A., and Nash, S.: Weather window analysis for the deployment, operation, and maintenance of marine renewable energy devices in Irish coastal waters, J. Ocean Eng. Mar. Energy, 10, 711–729, https://doi.org/10.1007/s40722-024-00340-2, 2024.

National Development Council Taiwan: Taiwan's pathway to net-zero emissions in 2050, available at: https://www.ndc.gov.tw/en/Content_List.aspx?n=B927D0EDB57A7A3A (last access: 26 January 2026), n.d.

National Oceanic and Atmospheric Administration, Climate Prediction Center: Oceanic Niño Index (ONI), Version 5 [data set], available at: https://origin.cpc.ncep.noaa.gov/products/analysis_monitoring/ensostuff/ONI_v5.php (last access: 1 September 2025), n.d.

National Oceanic and Atmospheric Administration, National Centers for Environmental Information: International Best Track Archive for Climate Stewardship (IBTrACS) [data set], available at: https://www.ncei.noaa.gov/products/international-best-track-archive (last access: 1 September 2025), n.d.

O'Brien, R. M.: A caution regarding rules of thumb for variance inflation factors, Qual. Quant., 41, 673–690, https://doi.org/10.1007/s11135-006-9018-6, 2007.

Rowell, D., Jenkins, B., Carroll, J., and McMillan, D.: How does the accessibility of floating wind farm sites compare to existing fixed bottom sites?, Energies, 15, 8946, https://doi.org/10.3390/en15238946, 2022.

Shimada, T., Chang, Y., and Lan, K.-W.: Climatological features of surface winds blowing through the Taiwan Strait, Int. J. Climatol., 36, 4287–4296, https://doi.org/10.1002/joc.4631, 2016.

Tseng, W.-L., Lin, C.-W., Wang, Y.-C., Hsu, H.-H., Chiu, K.-M., Wu, Y.-S., Hsieh, Y.-H., and Chen, Y.-T.: Evaluating constraints on offshore wind farm installation across the Taiwan Strait by exploring the influence of El Niño–Southern Oscillation on weather window assessment, Heliyon, 10, e40125, https://doi.org/10.1016/j.heliyon.2024.e40125, 2024.

https://doi.org/10.5194/wes-2026-121
Preprint. Discussion started: 4 September 2026

Wang, B., Wu, R., and Lau, K.-M.: Interannual variability of the Asian summer monsoon: contrasts between the Indian and the western North Pacific–East Asian monsoons, J. Climate, 14, 4073–4090, https://doi.org/10.1175/1520-0442(2001)014%3C4073:IVOTAS%3E2.0.CO;2, 2001.

Wilks, D. S.: Statistical Methods in the Atmospheric Sciences, 3rd edn., Academic Press, 2011.